EVALUATION OF CEMENT MATRIX HYDRATION PRODUCTS WITH X – RAY MICROTOMOGRAPHY IMAGES

Arthur Aviz Palma e Silva
PhD student in Civil Construction, University of Brasília | Brasília, Federal District | eng.aviz@gmail.com

Valdirene Maria Silva Capuzzo
Professor at the Department of Civil and Environmental Engineering, University of Brasília | Brasília, Federal District | valdirenemaria@unb.br

Mara Monaliza Linhares Pereira
PhD student in Civil Construction, University of Brasília | Brasília, Federal District | maramonaliza19@gmail.com

André Maués Brabo Pereira
Professor at the Department of Computer Science, Federal Fluminense University | Rio de Janeiro, Rio de Janeiro | andre@ic.uff.br

ABSTRACT

X-ray microtomography is widely used to investigate material properties due to its capacity to define distinct objects within specimens, often without requiring extraction from larger samples. In civil construction materials, this technique is extensively applied for determining pore properties, though challenges persist in evaluating complex regions such as hydration products in cementitious matrices. This study aimed to employ X-ray microtomography to quantify hydration products, focusing on C-S-H and CH phases. Cement paste samples were analyzed at 3, 7, and 28 days to compare hydration products across different ages and assess the technique's effectiveness. Microtomography images were captured at a resolution of 5µm. For image processing and segmentation, the Trainable Weka Segmentation tool in Fiji/ImageJ was employed, offering a guided workflow to implement machine learning-based segmentation of multidimensional images. The results demonstrated that the process could successfully identify and segment CH and C-S-H phases within the cement matrix, providing a practical tool for characterizing hydration products post-hydration. The findings highlight the potential of X-ray microtomography in advancing the analysis of hydration products in cementitious materials, paving the way for improved understanding of the microstructure and its evolution over time.

Keywords: X-ray microtomography; Segmentation; Cement matrix; Hydration products; Image processing.

INTRODUCTION

The X-ray microtomography technique allows visual inspection of defects, grains, minerals, fractures, cracks, and particularly the evaluation of voids in solid materials. Authors such as Rattanasak and Kendall (2005) employed the micro-CT technique to identify porosity and the characteristics of pores in cement mortars with pozzolanic compounds. However, there are several obstacles when using x-ray CT to analyze cementitious materials and concrete, including difficulties in accurately detecting hydrated phases due to poor image contrast in the solid phases and challenges related to the size of the sample and the spatial resolution of x-ray CT. Only a small number of researchers have utilized x-ray CT to measure the solid phases present in cement paste. Partial volume effects may occur as the voxel size grows larger, resulting in inaccuracies in image segmentation, particularly when dealing with a bulk system such as hydrated cement paste, void, or aggregate, noted by Provis et al. (2013). This study aimed to determine hydrated phases of calcium silicate hydrate and calcium hydroxide in X-ray microtomography samples, as well as differentiate them from other components of the cementitious matrix, such as pores and anhydrous cement. Image segmentation was performed with machine learning using Fiji/ImageJ software.

METHODOLOGY

This experiment was conducted using CP II-F40 cement, in accordance with ABNT NBR 16697 (2018). The mixture consisted solely of cement and water, with a water-to-cement ratio of 0.48. Cylindrical specimens (15 mm in diameter and 30 mm in height) were subjected to X-ray microtomography tests at 3, 7, and 28 days of age. The samples were scanned using a high-resolution X-ray micro-CT system (Zeiss Xradia Versa 510) at the Digital Materials Laboratory of the Federal Fluminense University (UFF). A total of 2000 images were acquired, from which 600 central images were selected as the region of interest to avoid artifacts commonly found in the top and bottom areas of micro-CT images. The scans were performed at a voxel resolution of 5 µm, chosen to maximize the analyzed sample volume. The image analysis procedure was based on the methodologies described by Enríquez-León et al. (2021) and Aboufoul & Garcia (2017).

The workflow was divided into three stages, with pre-processing of images, segmentation, and post-processing. The Fiji/ImageJ software was used as a tool to perform several stages of this experimental program, including the pre-processing of tomographic images. Firstly, histogram equalization was performed to redistribute the gray scale of pixels from natural images, Figure 1 a). The samples were transformed into 8bits, and their histogram was calibrated to follow the Fernandez (2008) reference for gray scale, as shown in Figure 1 b). An adjustment was made in histogram, in order to set the scale to became similar to Fernandez (2008) scale, so the products in the cement matrix would be determined with a reference. A filter was applied to improve image definition and reduce noise from the micro-CT acquisition process. The Non-local means denoising filter (NML) is a plug-in made for Fiji/ImageJ that provides this noise reduction and was used with parameters: sigma = 10 and smoothing factor = 1, Figure 1 c), according to Palma e Silva et al. (2022) and Buades et al. (2011).

Figure 1. Histogram correction and image normalization process with the non-local means filter, following the scale of Fernandez (2008).

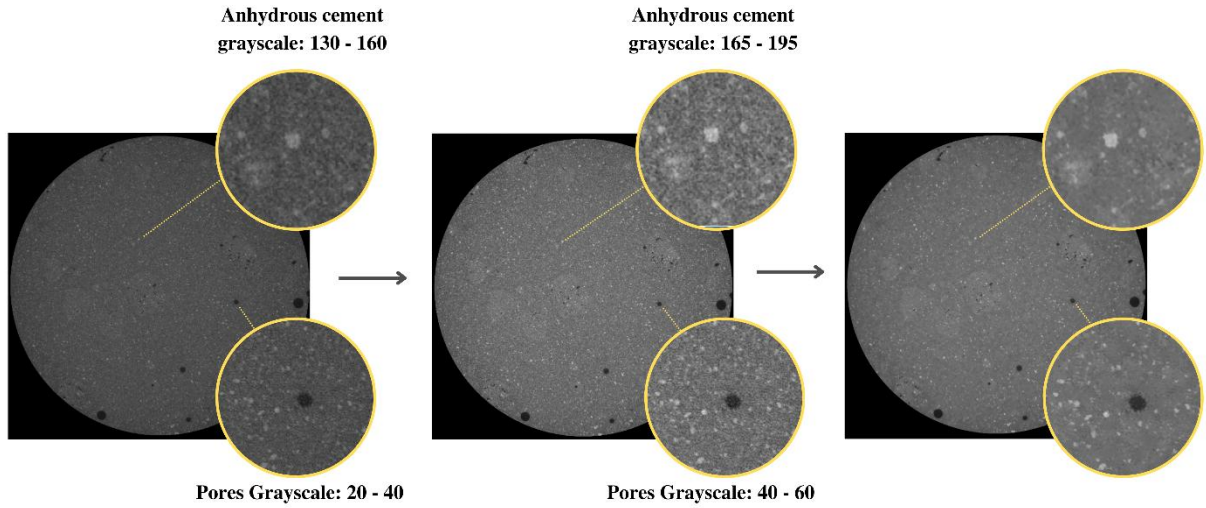

a) Natural image b) Histogram correction c) NML denoising filter

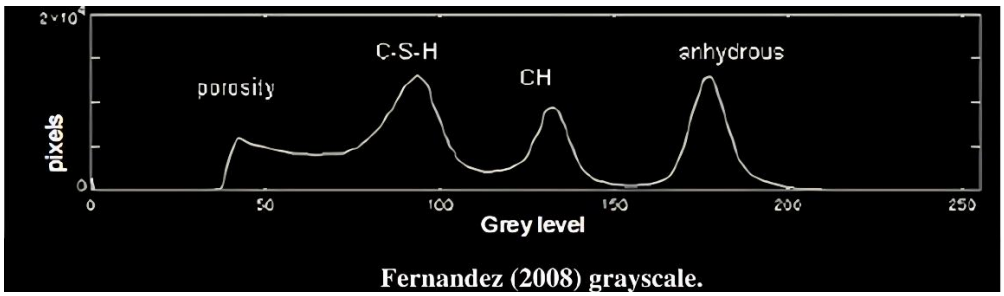

Source: Author (2025) and adapted from Fernandez (2008).

The Trainable Weka Segmentation plugin for Fiji/ImageJ, developed by Arganda-Carreras et al. (2017), combines manual segmentation and machine learning (ML) random forest algorithms. This tool was used to segment pores, C-S-H, CH, and anhydrous cement from the samples, as in Figure 2. After the training, each phase was selected, and the 3D visualizations of these 4 phases were possible and could be seen in Figure 3.

Figure 2. The Trainable Weka Segmentation plugin for Fiji/ImageJ. Determination of the pores, C-S-H, CH and anhydrous cement phases.

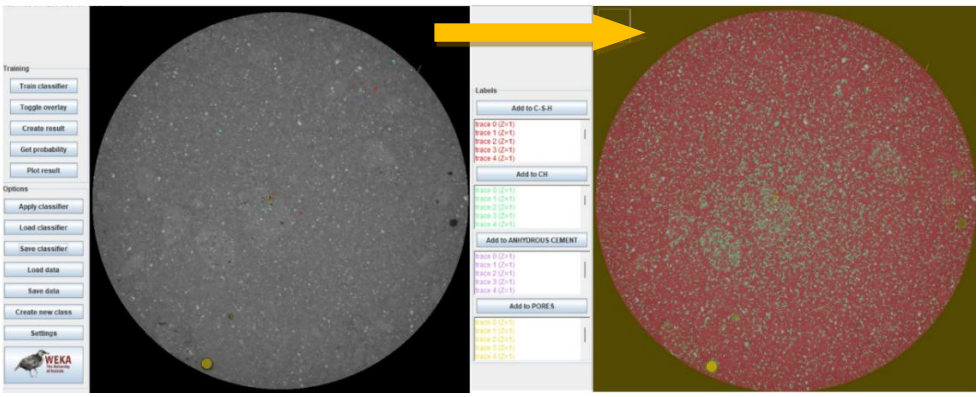

Source: Author (2025).

Figure 3. 3D visualizations of the cement matrix phases.

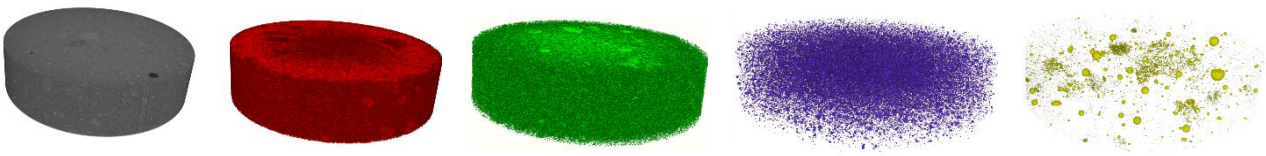

a) Cement Sample b) C – S - H c) $Ca(OH)_2$ d) Anhydrous Cement e) Porosity

Source: Author (2025).

After the segmentation of the micro-CT images, the percentage average of the phases was calculated across all analyzed images. The purpose of calculating the percentage average of each phase was to verify how the quantities of porosity, C-S-H, CH, and anhydrous cement differ as the cement hydration process progresses.

RESULTS AND DISCUSSIONS

After the quantitative analysis of the hydrated phases in the cementitious matrix, it was possible to understand how hydration progresses in the sample. The percentage results found for each age of C-S-H, CH, anhydrous cement, and porosity are contained in Figure 4. It can be observed that as the content of C-S-H and CH increases, the percentage of porosity and anhydrous cement decreases. The growth of hydration products occurs more pronouncedly in the first 7 days, but there is still an increase in the following days. The results are the averages of the 600 analyzed images that compose the micro – CT 3D reconstructions.

Figure 4. Comparison of the four cement matrix phases in the samples.

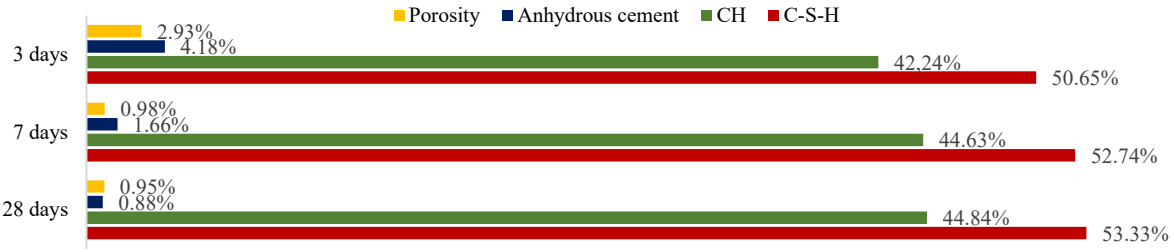

Source: Author (2025).

The measurement of calcium silicate hydrate (C-S-H) in the samples revealed an increase during the first days of hydration. Between 3 and 7 days, the C-S-H content increased by approximately 2.09%, while from 7 to 28 days, the growth was less pronounced, at only 0.59%. This indicates that most of the hydration process occurred within the first week.

The reduction in anhydrous cement content confirms this trend, decreasing significantly from 4.18% at 3 days to 1.66% at 7 days, and further to 0.88% at 28 days. Similarly, calcium hydroxide (CH) formation was more significant in the early stages, increasing from 42.24% at 3 days to 44.63% at 7 days. However, from 7 to 28 days, its content remained almost unchanged, reaching only 44.84%. This suggests that the CH production stabilized after the first week, reinforcing the idea that hydration slowed down over time. The porosity evolution follows this same pattern.

A reduction was observed from 3 to 7 days, dropping from 2.93% to 0.98%, indicating that hydration products filled part of the available pore space. However, after 7 days, the porosity remained nearly constant (0.98% at 7 days and 0.95% at 28 days), confirming that most of the pore refinement occurred in the initial period. These findings align with the expected hydration process of Portland cement, where the reaction rate is higher in the early stages and slows down over time as the available anhydrous cement decreases.

CONCLUSIONS

This study enabled the average evaluation of a cementitious matrix through Micro-CT. The results were satisfactory on a macroscopic analysis scale, however, studies with smaller voxel resolutions are necessary, as well as attempts to improve the micro – CT image contrast, in order to determine other phases like Aft and Afm, since their color are easily confounded with C-S-H phases. Also, the filler phases contained in cement may be assumed as anhydrous cement. Hence, the authors suggest as future studies, alternatives to better define the image contrast, in order to define Aft, Afm and filer phases in the test.

ACKNOWLEDGMENTS

We would like to express our gratitude to the Coordination for the Improvement of Higher Education Personnel (CAPES) and the National Council for Scientific and Technological Development (CNPq) for their financial support, and to the Digital Materials Laboratory at the Fluminense Federal University (UFF) for providing the facilities and technical assistance that were essential for the success of this research.

REFERENCES

RATTANASAK, U., & KENDALL, K. (2005). Pore structure of cement/pozzolan composites by X-ray microtomography. *Cement and Concrete Research*, 35(4), 637-640. Doi: https://doi.org/10.1016/j.cemconres.2004.04.022

PROVIS, J. L., HAJIMOHAMMADI, A., WHITE, C. E., BERNAL, S. A., MYERS, R. J., WINARSKI, R. P., ... & VAN DEVENTER, J. S. J. (2013). Nanostructural characterization of geopolymers by advanced beamline techniques. *Cement and Concrete Composites*, 36, 56-64. DOI: https://doi.org/10.1016/j.cemconcomp.2012.07.003

GALLUCCI, E., SCRIVENER, K., GROSO, A., STAMPANONI, M., & MARGARITONDO, G. (2007). 3D experimental investigation of the microstructure of cement pastes using synchrotron X-ray microtomography (μCT). *Cement and Concrete Research*, 37(3), 360-368. DOI: https://doi.org/10.1016/j.cemconres.2006.10.012

ENRÍQUEZ-LEÓN, A. J., DE SOUZA, T. D., ARAGÃO, F. T. S., PEREIRA, A. M. B., & NOGUEIRA, L. P. (2021). Characterization of the air void content of fine aggregate matrices within asphalt concrete mixtures. *Construction and Building Materials*, 300, 124214. DOI: https://doi.org/10.1016/j.conbuildmat.2021.124214

ABOUFOUL, M., & GARCIA, A. (2017). Factors affecting hydraulic conductivity of asphalt mixture. *Materials and Structures*, 50, 1-16. DOI: https://doi.org/10.1617/s11527-016-0982-6

FERNÁNDEZ, M. M. (2008). Effect of particle size on the hydration kinetics and microstructural development of tricalcium silicate. *EPFL*. DOI: http://dx.doi.org/10.5075/epfl-thesis-4102

PALMA E SILVA, A. A. P., CAPUZZO, V. M. S., SILVA, E. F., PEREIRA, A. M. B., & E SILVA, D. A. P. (2022). Evaluation of mechanical properties and microstructure of high-performance mortars with superabsorbent polymers and metakaolin by means of X-ray computed microtomography. *Journal of Building Engineering*, 51, 104219. DOI: https://doi.org/10.1016/j.jobe.2022.104219